Homogenization Method Based on Cauer Ladder Network Representation of Unit Cell

Shingo Hiruma[1], *Member, IEEE*, Yasuhito Takahashi[2], *Member, IEEE*, and Tetsuji Matsuo[1], *Member, IEEE*

[1]Graduate School of Engineering, Kyoto University, Kyoto, 615-8510, Japan
[2]Department of Electrical Engineering, Doshisha University, Kyoto, 615-8510, Japan

In this study, a novel homogenization method based on the B-input Cauer ladder network method, which is a new variant of the CLN method, is proposed. This method yields complex permeability in the form of a continued fraction, which is deemed the impedance function of the Cauer circuit and can be instantly applied to time-domain analysis. By guaranteeing all the positive circuit parameters in the Cauer circuit through the CLN algorithm, this method proved to be robust and stable for time-domain analysis.

***Index Terms*—Complex permeability, Cauer ladder network method, homogenization method, unit cell approach.**

I. INTRODUCTION

To suppress eddy currents, electromagnetic devices employ materials with fine structures such as laminated steel sheets, Litz wires, copper foils, and dust cores. To enhance the efficiency of these devices, it is crucial to accurately assess the eddy-current losses that occur within fine structures. However, conventional methods, such as the finite element method (FEM), require spatial discretization that considers fine structures, resulting in a massive number of unknowns throughout the analysis domain.

The use of homogenization methods [1]-[5] can significantly reduce the computational costs associated with multiscale problems. In the homogenization method, fine structures are modeled as bulks and their material properties are represented by complex permeabilities. The complex permeability is determined such that the influence and losses of eddy currents in fine structures are correctly represented from a macroscopic viewpoint. Methods for obtaining complex permeability include a numerical method using unit cell analysis [1][3], an analytical method based on continued fraction expansion [2], a semi-analytical method using the extended Ollendorff formula [2], and a method based on the model order reduction (MOR) technique to obtain an equivalent circuit model [4][5]. In the MOR method [4], the Cauer circuit is obtained as an equivalent circuit model for complex permeability, which is advantageous for time-domain analysis. However, it is known that the circuit parameters of the Cauer circuit can become negative owing to the numerical instability. Because the passivity of the circuit is not ensured owing to the negative circuit parameters, the robustness of time-domain analysis is low.

In this study, we propose a novel homogenization method based on the newly developed B-input Cauer Ladder Network (CLN) method, which is a new variant of the CLN method [6]. Because the CLN method generates all the positive circuit parameters, the robustness in the time-domain analysis is improved compared with the existing method of calculating complex permeability [4]. In addition, the CLN method can be truncated to the desired accuracy by using error estimation methods [7].

Manuscript received April XX, 20XX; revised May XX, 20XX and June XX, 20XX; accepted July XX, 20XX. Date of publication July 10, 20XX; date of current version July XX, 20XX. Corresponding author: S. Hiruma (e-mail: hiruma.shingo.3w@kyoto-u.ac.jp).

Color versions of one or more of the figures in this paper are available online at http://ieeexplore.ieee.org.

Digital Object Identifier (inserted by IEEE).

II. HOMOGENIZATION METHOD BASED AND MODEL ORDER REDUCTION METHOD

In the unit cell method, we assume that the fine structure of interest is composed of spatially periodic unit cell Ω. After solving the eddy current problems in the unit cell where a uniform external time-harmonic magnetic flux density $\boldsymbol{B}_0$ is given, the complex permeability $\langle\dot{\mu}\rangle$ is evaluated by

$$\langle\dot{\mu}\rangle = \frac{\int_\Omega |\boldsymbol{B}_0|^2 d\Omega}{\int_\Omega \nu |\boldsymbol{B}|^2 d\Omega - \dfrac{1}{j\omega}\int_\Omega \sigma |\boldsymbol{E}|^2 d\Omega} \tag{1}$$

where $\boldsymbol{B}, \boldsymbol{E}, \nu, \omega, \sigma$ and j denote the magnetic flux density, electric field, reluctivity, angular frequency, conductivity, and imaginary unit, respectively. To enhance the availability of the evaluated complex permeability, the MOR method was employed to obtain an analytical expression for the frequency-dependent function in the form of a continued fraction using the Cauer via Lanczos algorithm (CVL), which is a bi-Lanczos-based algorithm [4]. Because the continued fraction can be regarded as the impedance of the Cauer circuit, time-domain analysis can be performed by coupling the system with the circuit equation. However, this method does not ensure the passivity of the reduced-order system, because it may generate negative circuit parameters in the Cauer circuit. Thus, we investigated the use of the CLN method to improve stability and establish a robust algorithm.

III. FORMULATION

The CLN method [6] reduces the distribution of the electromagnetic field to a Cauer ladder network with a small number of lumped parameters. There are two main types of CLN methods: H- and E-input. In the H-input version, the field is excited through the tangential component of the magnetic field under the Neumann boundary condition, whereas in the E-input version, the field is excited through the normal component of the electric field under the Dirichlet boundary condition. However, a flux input version of the CLN method has not yet been proposed. In this section, we formulate the newly developed B-input CLN method by deriving the admittance function for eddy current problems.

A. B-input CLN Method

Let us consider a linear eddy current problem in which the field is excited with a time-harmonic unit magnetic flux $\Phi_{-1} = 1$ [Wb], as shown in Fig. 1.

$$\nabla \times \nu \nabla \times \boldsymbol{A} + j\omega\sigma\boldsymbol{A} = 0, \qquad \text{in } \Omega, \tag{2}$$

$$\boldsymbol{A} \times \boldsymbol{n} = \boldsymbol{0}, \qquad \text{on } \Gamma_D, \tag{3}$$

$$\boldsymbol{H} \times \boldsymbol{n} = \boldsymbol{0}, \qquad \text{on } \Gamma_{\text{in}}, \Gamma_{\text{out}} \tag{4}$$

$$\int_{\Gamma_{\text{in}}} \boldsymbol{B} \cdot \boldsymbol{n} dS = \Phi_{-1} = 1 \tag{5}$$

where $\boldsymbol{A}$ and $\boldsymbol{H}$ denote the magnetic vector potential and magnetic field and $\boldsymbol{n}$ represents the normal unit vector on the boundary. Because we consider a linear problem, all material parameters are constants. Γ_D is the Dirichlet boundary condition on which the unit magnetic flux is imposed, and $\Gamma_{\text{in}}, \Gamma_{\text{out}}$ denote the Neumann boundary condition. With these boundary conditions, we first obtain the magnetostatic field by solving

$$\nabla \times \boldsymbol{H}_{-1} = \boldsymbol{0}, \qquad \text{in } \Omega. \tag{6}$$

Let the solution $\boldsymbol{A}_{-1}$ satisfy $\boldsymbol{H}_{-1} = \nu\nabla \times \boldsymbol{A}_{-1}$. Then, the total field of the magnetic field and vector potentials can be decomposed into the static field part $\boldsymbol{H}_{-1}, \boldsymbol{A}_{-1}$ and the response field part $\widetilde{\boldsymbol{H}}, \widetilde{\boldsymbol{A}}$ as follows

$$\boldsymbol{H} = \boldsymbol{H}_{-1} + \widetilde{\boldsymbol{H}}, \qquad \boldsymbol{A} = \boldsymbol{A}_{-1} + \widetilde{\boldsymbol{A}}. \tag{7}$$

The boundary conditions for $\widetilde{\boldsymbol{H}}$ and $\widetilde{\boldsymbol{A}}$ are

$$\widetilde{\boldsymbol{A}} \times \boldsymbol{n} = 0, \qquad \text{on } \Gamma_D, \tag{8}$$

$$\widetilde{\boldsymbol{H}} \times \boldsymbol{n} = \boldsymbol{0}, \qquad \text{on } \Gamma_{\text{in}}, \Gamma_{\text{out}}. \tag{9}$$

With these notations, the governing equation becomes

$$\nabla \times \nu \nabla \times \widetilde{\boldsymbol{A}} + j\omega\sigma\widetilde{\boldsymbol{A}} = -j\omega\sigma\boldsymbol{A}_{-1} = \sigma\boldsymbol{E}_{-1}, \qquad \text{in } \Omega \tag{10}$$

where $\boldsymbol{E}_{-1} = -j\omega\boldsymbol{A}_{-1}$. The power is then calculated as

$$\begin{aligned} P &= \frac{j\omega}{2}\int_\Omega \nu|\boldsymbol{B}|^2 \mathrm{d}\Omega + \frac{1}{2}\int_\Omega \sigma|\boldsymbol{E}|^2 \mathrm{d}\Omega \\ &= \frac{j\omega}{2}\int_\Omega \boldsymbol{B}_{-1} \cdot \boldsymbol{H}_{-1}^* \,\mathrm{d}\Omega + \frac{1}{2}\int_\Omega \boldsymbol{E}_{-1} \cdot \sigma\left(\boldsymbol{E}_{-1} + \widetilde{\boldsymbol{E}}\right)^* \mathrm{d}\Omega, \end{aligned} \tag{11}$$

where we used $\widetilde{\boldsymbol{E}} = -j\omega\widetilde{\boldsymbol{A}}$. Because the unit flux $\Phi_{-1} = 1$ flows through the domain, the induced voltage becomes $V = -j\omega\Phi_{-1} = -j\omega$. Therefore, admittance can be written as $Y^* = 2P/V^2 = 2P/\omega^2$. The finite element discretization of the governing equation (10) results in

$$(K + sN)\widetilde{\boldsymbol{a}} = -sN\boldsymbol{a}_{-1}^\star \tag{12}$$

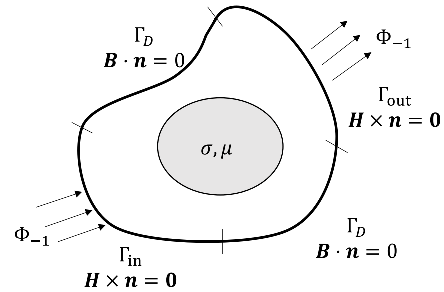

Fig. 1. Analysis domain where eddy currents are excited by a time-harmonic external magnetic flux Φ_{-1}.

where $s = j\omega$ and K, N are positive definite matrices. The vector potential $\boldsymbol{a}_{-1}^\star$ denotes the discretized vector potential $\boldsymbol{A}_{-1}$. Using these notations, we obtain the discretized expression of the admittance function (11) as follows

$$\begin{aligned} Y = \frac{2P^*}{\omega^2} &= \frac{(\boldsymbol{a}_{-1}^\star, \boldsymbol{a}_{-1}^\star)_K}{s} + (\boldsymbol{a}_{-1}^\star, \widetilde{\boldsymbol{a}} + \boldsymbol{a}_{-1}^\star)_N \\ &= \frac{(\boldsymbol{a}_{-1}^\star, \boldsymbol{a}_{-1}^\star)_K}{s} + \boldsymbol{a}_{-1}^{\star\,\top} K(K + sN)^{-1} N\boldsymbol{a}_{-1}^\star \end{aligned} \tag{13}$$

The bilinear functions $(\boldsymbol{x}, \boldsymbol{y})_K = \boldsymbol{x}^\top K\boldsymbol{y}, (\boldsymbol{x}, \boldsymbol{y})_N = \boldsymbol{x}^\top N\boldsymbol{y}$ introduced here are related to the energy norms of the magnetic and electric fields, respectively. The second term can be expanded into a continued fraction using Algorithm A2 (see Appendix), and the first term can be defined as $L_{-1} = (\boldsymbol{a}_{-1}^\star, \boldsymbol{a}_{-1}^\star)_K^{-1}$, which represents the excitation inductance. Therefore, we have

$$Y = \frac{1}{sL_{-1}} + \cfrac{1}{R_0 + \cfrac{1}{\cfrac{1}{sL_1} + \cfrac{1}{R_2 + \cfrac{1}{\ddots}}}}. \tag{14}$$

The entire process for obtaining the continued fraction expansion leads to the B-input CLN method as follows:

B-input CLN method

Solve a magneto-static equation with unit external flux $\Phi_{-1} = 1$ Wb

$$K\boldsymbol{a}_{-1}^\star = \boldsymbol{b}\Phi_{-1}, L_{-1} = (\boldsymbol{a}_{-1}^\star, \boldsymbol{a}_{-1}^\star)_K^{-1}$$

Set

$$\boldsymbol{e}_0 = \boldsymbol{a}_{-1}^\star, R_0 = (\boldsymbol{e}_0, \boldsymbol{e}_0)_N^{-1}$$
$$\boldsymbol{a}_{-1} = 0$$

For $n = 1,2, \ldots$ do

$$K\boldsymbol{a}_{2n-1} = K\boldsymbol{a}_{2n-3} + R_{2n-2}N\boldsymbol{e}_{2n-2}$$
$$L_{2n-1} = (\boldsymbol{a}_{2n-1}, \boldsymbol{a}_{2n-1})_K$$
$$\boldsymbol{e}_{2n} = \boldsymbol{e}_{2n-2} - L_{2n-1}^{-1}\boldsymbol{a}_{2n-1}$$
$$R_{2n} = (\boldsymbol{e}_{2n}, \boldsymbol{e}_{2n})_N^{-1}$$

End

It should be emphasized that the algorithm is different from both the H- and E-input CLN methods in terms of the calculation of excitation inductance. Note that in the case of 3-D analysis where the matrix K is semi-definite, the algorithm is modified to correct the divergence of the CLN basis function.

The bases $\boldsymbol{a}_{2n-1}, \boldsymbol{e}_{2n-2}, n \geq 1$ are the orthogonal basis with respect to energy norms [6]. In addition, the bases $\boldsymbol{a}_{2n-1}, n \geq 1$ obtained by the CLN method and the initial basis $\boldsymbol{a}^{\star}_{-1}$ are orthogonal with respect to the energy norm, which can readily be checked as follows

$$(\boldsymbol{a}_{2n-1}, \boldsymbol{a}^{\star}_{-1})_K = \int_{\Omega} \boldsymbol{B}_{2n-1} \cdot \boldsymbol{H}_{-1}\, \mathrm{d}\Omega$$
$$= \int_{\partial\Omega} \boldsymbol{A}_{2n-1} \times \boldsymbol{H}_{-1} \cdot \boldsymbol{n} d\Gamma + \int_{\Omega} \boldsymbol{A}_{2n-1} \cdot \nabla \times \boldsymbol{H}_{-1} d\Omega = 0. \quad (15)$$

where the first term vanishes because of the boundary conditions for bases (3), (4), (8), and (9), and the second term vanishes because of (6).

B. Robustness and stability

In the CLN method, the circuit parameters satisfy

$$L_{2n-1} = (\boldsymbol{a}_{2n-1}, \boldsymbol{a}_{2n-1})_K \geq 0, \qquad n = 0,1,2,\ldots \qquad (16)$$
$$R_{2n} = (\boldsymbol{e}_{2n}, \boldsymbol{e}_{2n})_N^{-1} \geq 0, \qquad n = 1,2,3,\ldots \qquad (17)$$

because K, N are positive (semi-) definite matrices, which implies that no negative circuit parameters, that act as active elements, are included in the Cauer circuit. This ensures the passivity of the Cauer circuit, and that the system is robust and stable for arbitrary input. This property is significant when we consider the time-domain analysis.

C. Error estimation

Another advantage of using the CLN method for homogenization is the use of error estimation methods [7]. For example, by designating the maximum frequency $f_{\max}$ and desired accuracy α, the number of ladder stages in the CLN method can be truncated if the following criterion is satisfied

$$\frac{\epsilon_e}{d_e} < \alpha \qquad (18)$$

where $d_e = \|(\boldsymbol{E}' + \boldsymbol{E})/2\|_N, \epsilon_e = \|\boldsymbol{E}' - \boldsymbol{E}\|_N$. The electric fields $\boldsymbol{E}, \boldsymbol{E}'$ are the reconstructed fields obtained using the CLN basis function [7]. This criterion ensures the accuracy of the complex permeability for frequencies $f \leq f_{\max}$.

D. Application to homogenization method

As an application of the B-input CLN method, we consider a unit cell consisting of a conductor and air region [3]. An external uniform magnetic flux density is applied to excite the field, which can be interpreted as the main magnetic flux Φ_{-1} flowing through the excitation inductance in the Cauer circuit. For a 2D unit cell Ω with size $2d \times 2w$ in the xy-plane, the boundary conditions for applying a unit magnetic flux $\Phi_{-1} = 1$ Wb in the y direction would be

$$A_z = A_+ = -1/2, \qquad \text{on } \Gamma_+, \qquad (19)$$
$$A_z = A_- = 1/2, \qquad \text{on } \Gamma_- \qquad (20)$$

where Γ_+ is the boundary at $x = d$, and Γ_- is at $x = -d$.

The complex magnetic reluctivity of the unit cell is obtained with the B-input CLN method as follows

TABLE 1 LUMPED CIRCUIT PARAMETERS OBTAINED BY CLN AND CVL METHODS FOR A UNIT CELL $a = 1\ mm,\ \mu_r = 1$

	$\tilde{L}_{2n-1}$		$\tilde{R}_{2n}$	
n	CLN	CVL	CLN	CVL
0	1.000×10^{0}	1.000×10^{0}	3.5529×10^{-6}	3.55×10^{-6}
1	2.895×10^{0}	2.895×10^{0}	1.5289×10^{-7}	1.53×10^{-7}
2	1.288×10^{1}	1.288×10^{1}	2.1499×10^{-8}	2.15×10^{-8}
3	3.521×10^{1}	3.521×10^{1}	5.2232×10^{-9}	5.22×10^{-9}
4	7.477×10^{1}	7.477×10^{1}	1.7304×10^{-9}	1.75×10^{-9}
5	1.365×10^{2}	4.562×10^{2}	7.0315×10^{-10}	7.61×10^{-8}
6	5.751×10^{2}	1.937×10^{2}	5.2756×10^{-8}	6.99×10^{-10}
7	3.684×10^{2}	2.266×10^{2}	3.2479×10^{-10}	4.65×10^{-10}
8	3.471×10^{2}	8.263×10^{3}	2.1897×10^{-10}	1.02×10^{-9}
9	1.377×10^{4}	3.594×10^{2}	6.6911×10^{-10}	2.14×10^{-10}
10	5.311×10^{2}	2.612×10^{3}	2.1290×10^{-10}	3.46×10^{-10}
11	7.467×10^{3}	-8.803×10^{3}	1.7069×10^{-10}	-1.11×10^{-9}
12	2.750×10^{3}	5.429×10^{2}	1.0943×10^{-9}	3.95×10^{-11}
13	1.571×10^{3}	-1.838×10^{5}	1.6160×10^{-9}	-1.13×10^{-10}
14	4.277×10^{3}	-1.375×10^{5}	2.0232×10^{-10}	-1.87×10^{-10}
15	1.941×10^{4}	7.927×10^{2}	1.7350×10^{-9}	1.28×10^{-10}
16	7.312×10^{3}	1.287×10^{4}	3.8215×10^{-10}	1.03×10^{-9}
17	4.912×10^{3}	-1.998×10^{3}	7.4401×10^{-11}	-4.87×10^{-9}

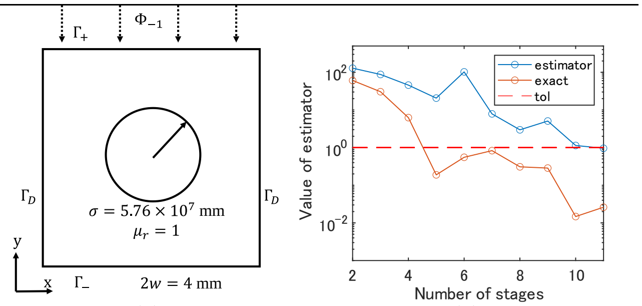

(a) (b)

Fig. 2 (a)Unit cell model and (b) Error estimator and exact relative error plotted against number of the ladder stages for a unit cell $a = 1$ mm, $\mu_r = 1$ with $f_{\max} = 10^6$ Hz, $\alpha = 0.01$.

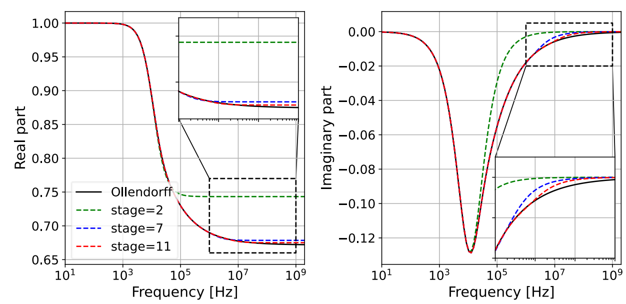

Fig.3 Frequency characteristics of complex permeability obtained using CLN method and Ollendorff formula [2].

$$\frac{j\omega}{2} \int_{\Omega} \langle \dot{\nu} \rangle^* |B_0|^2 d\Omega = P = \frac{\omega^2 Y^*}{2},$$
$$\langle \dot{\nu} \rangle = \langle \dot{\mu} \rangle^{-1} = \frac{sY}{\int_{\Omega} |B_0|^2 d\Omega} = s\left(\frac{d}{w}\right) Y \qquad (21)$$

which has the form of a continued fraction.

IV. NUMERICAL ANALYSIS

We consider a 2-D square unit cell Ω of size $2w \times 2w$ with $w = 2$ mm, as shown in Fig. 2a. At the center of the unit cell, we considered a conductor radius $a = 1$ mm, conductivity $\sigma = 5.76 \times 10^7$ S/m, and relative permeability of 1. Table 1 lists the circuit parameters calculated using the CLN and CVL [4] methods for this unit cell model. Here, $\tilde{L}_{2n+1} = L_{2n+1}/\mu_0$, $\tilde{R}_{2n} = \mu_0 R_{2n}$ are normalized values. The CVL method yields negative values for $\tilde{L}_{21}$, $\tilde{R}_{22}$ and so on whereas all circuit parameters obtained by the CLN method are positive.

Next, we apply the truncation algorithm described in Sec. III-C. Setting the maximum frequency and required accuracy to $(f_{\max}, \alpha) = (10^6\ \text{Hz}, 0.01)$, Fig. 2b shows the evolution of the estimated error $\epsilon_e/d_e \times 100$ and exact relative error with respect to the number of ladder stages. The required accuracy was achieved after 11 ladder stages, with an exact relative error of 0.03% at that point. The error tends to decrease but exhibits local fluctuations. Additionally, the estimated error always provided an upper bound for the exact error. The frequency characteristics of complex permeability for different numbers of ladder stages are shown in Fig. 3 where the complex permeability obtained from the Ollendorff formula are also plotted. As the number of ladder stages increased, the characteristics converged.

Acknowledgment

This work was supported in part by the JSPS KAKENHI Grant Numbers 22K14237 and 24K17261.

Appendix

Two algorithms for the continued fraction expansion of the impedance and admittance, which are equivalent to the H-input and E-input CLN methods [6], are shown here. The H-input CLN method performs a continued fraction expansion of the impedance function around $s = 0$, whereas the E-input CLN method performs an expansion of the admittance function around $s = 0$. This corresponds to a similar algorithm: the Padé approximation in moment-matching MOR [8].

A. H-input CLN method

First, we consider the H-input version of the CLN method that performs the continued fraction expansion of the transfer function below

$$Z = s\boldsymbol{b}^{\top}(K + sN)^{-1}\boldsymbol{b} \tag{22}$$

where K, N are n-dimensional positive definite matrices, $\boldsymbol{x}, \boldsymbol{b}$ are the unknown vector and right-handed side vector, respectively, and s is the complex frequency. The following continued fraction expansion can be performed using Algorithm A1:

$$Z = s\boldsymbol{b}^{\top}(K + sN)^{-1}\boldsymbol{b} = \cfrac{1}{\cfrac{1}{sL_1} + \cfrac{1}{R_2 + \cfrac{1}{\cfrac{1}{sL_3} + \cfrac{1}{\ddots}}}}. \tag{23}$$

As discussed in Sec. III-A, in the case of a semi-definite matrix K, for example 3-D electromagnetic FEM using edge elements, the algorithm is modified to regularize the CLN basis function.

Algorithm A1 (H-input CLN method)

Set

$$\boldsymbol{a}_1 = K^{-1}\boldsymbol{b}, L_1 = (\boldsymbol{a}_1, \boldsymbol{a}_1)_K, \boldsymbol{e}_0 = 0$$

For $n = 1,2, \ldots$ do

$$\boldsymbol{e}_{2n} = \boldsymbol{e}_{2n-2} - L_{2n-1}^{-1}\boldsymbol{a}_{2n-1}$$
$$R_{2n} = (\boldsymbol{e}_{2n}, \boldsymbol{e}_{2n})_N^{-1}$$
$$K\boldsymbol{a}_{2n+1} = K\boldsymbol{a}_{2n-1} + R_{2n}N\boldsymbol{e}_{2n}$$
$$L_{2n+1} = (\boldsymbol{a}_{2n+1}, \boldsymbol{a}_{2n+1})_K$$

End

B. E-input CLN method

Next, we consider the E-input version of the CLN method that performs the continued fraction expansion of the transfer function

$$Y = \boldsymbol{b}^{\top}K(K + sN)^{-1}N\boldsymbol{b}. \tag{24}$$

Typically, it appears as the admittance of an electromagnetic system. This also appears in the B-input CLN method discussed in this study. Continued fraction expansion for the function Y can be performed using Algorithm A2:

$$Y = \boldsymbol{b}^{\top}K(K + sN)^{-1}N\boldsymbol{b} = \cfrac{1}{R_0 + \cfrac{1}{\cfrac{1}{sL_1} + \cfrac{1}{R_2 + \cfrac{1}{\ddots}}}}. \tag{25}$$

Algorithm A2 (E-input CLN method)

Set

$$\boldsymbol{e}_0 = \boldsymbol{b}, R_0 = (\boldsymbol{e}_0, \boldsymbol{e}_0)_N^{-1}$$
$$\boldsymbol{a}_{-1} = 0$$

For $n = 1,2, \ldots$ do

$$K\boldsymbol{a}_{2n-1} = K\boldsymbol{a}_{2n-3} + R_{2n-2}N\boldsymbol{e}_{2n-2}$$
$$L_{2n-1} = (\boldsymbol{a}_{2n-1}, \boldsymbol{a}_{2n-1})_K$$
$$\boldsymbol{e}_{2n} = \boldsymbol{e}_{2n-2} - L_{2n-1}^{-1}\boldsymbol{a}_{2n-1}$$
$$R_{2n} = (\boldsymbol{e}_{2n}, \boldsymbol{e}_{2n})_N^{-1}$$

End

References

[1] J. Gyselinck, R. V. Sabariego, and P. Dular, “A Nonlinear Time-domain Homogenization Technique for Laminated Iron Cores in Three-dimensional Finite-element Models,” *IEEE Trans. Magn.*, vol. 42, no. 4, pp. 763-766, Apr. 2006.

[2] H. Igarashi, “Semi-Analytical Approach for Finite-Element Analysis of Multi-Turn Coil Considering Skin and Proximity Effects,” *IEEE Trans. Magn.*, vol. 53, no. 1, Art no. 7400107, Jan. 2017.

[3] A. D. Podoltsev, I. N. Kucheryavaya and B. B. Lebedev, "Analysis of Effective Resistance and Eddy-Current Losses in Multiturn Winding of High-Frequency Magnetic Components," *IEEE Trans. Magn.*, vol. 39, no. 1, pp. 539-548, Jan. 2003.

[4] S. Hiruma and H. Igarashi, “Homogenization Method Based on Cauer Circuit via Unit Cell Approach,” *IEEE Trans. Magn.*, vol. 56, no. 2, Art no. 7505805, Feb. 2020.

[5] Y. Sato and H. Igarashi, “Time-Domain Analysis of Soft Magnetic Composite Using Equivalent Circuit Obtained via Homogenization,” *IEEE Trans. Magn.*, vol. 53, no. 6, Art no. 7402204, June 2017.

[6] A. Kameari, H. Ebrahimi, K. Sugahara, Y. Shindo, and T. Matsuo, “Cauer Ladder Network Representation of Eddy-current Fields for Model Order Reduction Using Finite Element Method,” *IEEE Trans. Magn.*, vol. 54, no. 3, Art no. 7201804, 2018.

[7] S. Hiruma, S. Clénet, H. Igarashi and T. Henneron, "Error Estimator for Cauer Ladder Network Representation," *IEEE Trans. Magn.*, vol. 58, no. 9, Art no. 7500904, Sept. 2022.

[8] D. Rafiq and M.A. Bazaz, “Model Order Reduction via Moment-Matching: A State of the Art Review,” *Arch Computat Methods Eng* 29, 1463–1483 2022.